

Glass clarified as the Self-Organizing System

Elena A. Chechetkina

Institute of General and Inorganic Chemistry of Russian Academy of Sciences (1980-2011)

Moscow, Russia

eche2010@yandex.ru

Abstract – The term “self-organization” in contemporary glass science relates usually to the “intermediate phase” in frames of the *topological constraint theory* of glass structure. This theory, however, has no a relation to classical theory of self-organization – synergetics. The synergetic approach proposed here is based on characteristic instability of chemical bonding in the form of the *bond wave* representing the spatiotemporal correlation between elementary acts of bond exchange. In frames of the model, glass transition is considered as the *dimensionality transition*: from 3D bond wave in glass-forming liquid to 2D bond wave in glass. The model explains characteristic *hierarchical structure*, including non-crystalline long-range order, the *semi-deterministic* behavior of properties, and a role of *information fields* for adaptation of glassy material to a current medium.

Keywords: *glass, self-organization, chemical bonding, glass transition, glass structure, glass-forming liquid, viscosity, fractography, information field*

I. INTRODUCTION

Glass articles accompany us everywhere – from windows and kitchenware to fiber communications and active elements for electronic devices. At the same time no one material is so enigmatic, when even the nature of glass transition remains a subject of incessant discussions. To my opinion, this scientific mist appears due to ignoring of self-organization, a wide-spread feature of many objects observed everywhere: in physics, chemistry, biology, psychology, sociology, etc. [1-3].

My understanding glass as the self-organizing system began in 1980s in the laboratory of *S. A. Dembovsky*, who just created a new theory of glass formation from the chemical bond point of view. The core of his theory were special bonds in the form of *hypervalent* species, which were considered initially as “defects” in covalent network [4] and then as a necessary element of glass structure, an element that ensures both glass properties and glass formation phenomenon at all [5]. During our search of these “glassy” bonds by viscous flow in magnetic fields [6,7], the *bond wave* model, which considers a collective behavior of the “glassy” bonds as a spatiotemporal process, was born.

The model was successively applied then for explanation of other glass features, both the known ones (medium-range order, non-Arrhenius viscosity, specific fracture) and those discovered by action of weak *information fields* (magnetic,

ultrasound, etc.). Below there is a short summary of the bond wave model history, present status and perspective.

II. DISSIPATIVE PATTERN – THE BOND WAVE

Glass is understood usually as the *bulk non-crystalline material obtained by cooling of melt and then supercooled liquid up to its solidification* [8,9]. Corresponding process is shown schematically in **Fig.1**, where T_g , T_m , T_b , and T_m^* are the glass transition temperature, melting point, boiling point, and a “normal” melting point clarified some below (see **Table 1**).

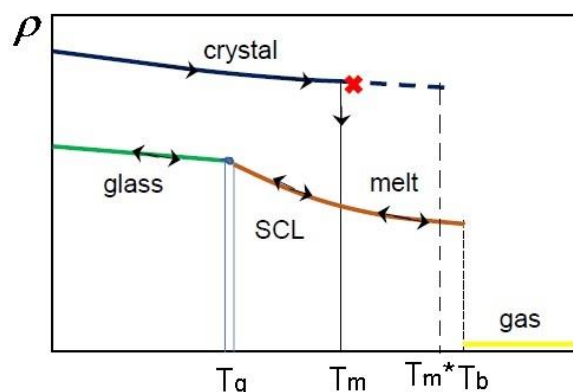


Figure 1. Density-temperature diagram for the crystal-melt-glass transformations; SCL is supercooled liquid.

Typical inorganic glasses belong to oxides (SiO_2 , B_2O_3 , etc.) or chalcogenides (Se , As_2S_3); both groups are based on **covalent bonds**, e.g., Si–O for SiO_2 or As–S for As_2S_3 . Conventional **continuous random network (CRN)** model of glass structure [10] operates with the same covalent bonds in glass and crystal. For example, in both crystalline and glassy SiO_2 each O-atom forms two covalent bonds with its neighbors, so being *two-coordinated* (O_2), and each Si-atom is *four-coordinated* (Si_2). This means that CRN operates with the **short-range order (SRO)**, and there is no a difference between SRO in glassy and crystalline states of a substance.

Classical CRN in **Fig.2a** corresponds to the B_2O_3 -like network consisting of B_3 and O_2 atoms. Such a CRN, however, cannot realize “in bulk” because of characteristic *rigidity* of covalent bond, which can change the bond length and valence angles only in narrow limits, a fact that makes classical CRN unstable after few random conjunctions.

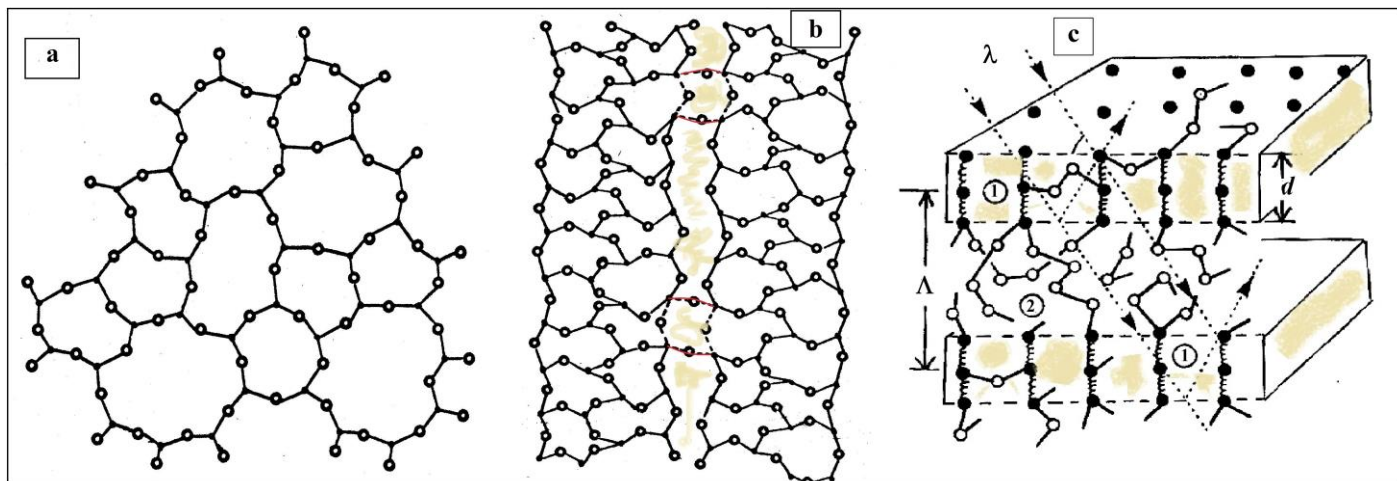


Figure 2. Models for glass structure after (a) Zachariasen [10], (b) Robinson [11] and (c) Chechetkina [12].

To overcome this shortcoming of CRN, Robinson [11] has introduced into CRN the “cuts” populated with weak/flexible bonds (Fig.2b), thus tailoring rigid covalent fragments with the following increase of CRN stability. The notions about some “weak bonds” emerge periodically in glass literature (see, e.g., Ref.13); however, without appropriate justification of the bonds’ nature.

Two other ways for reconstruction of classical CRN concern either special junction of covalent bonds such as “outrigger rafts” after Phillips [14] or the **topological constraint theory** of glass structure [15-17]. The theory considers only “normal” atomic coordination (i.e., Si₄, O₂, As₃, Se₆, etc.) which are used for calculation of the *average coordination number* $\langle r \rangle$ in accord with chemical composition of a system. The obtained $\langle r \rangle$ is compared with “magic” coordination number $\langle r \rangle^* = 2.4$ which corresponds to the free-of-stress state of a network. Really, the composition-property dependencies in binary glass-forming systems demonstrate anomaly in the region around corresponding “magic” composition; just this known as “**intermediate phase**” [18] is compared with the *self-organization* phenomenon in glass.

In my model, self-organization is a basic feature of the glassy state irrespectively of a concrete glass composition. The bond wave model naturally combines “weak bonds” and “self-organization” owing to the *two-state* chemical bonding and a collective *feedback* between the states in the form of the **bond wave** representing spatiotemporal correlation between elementary acts of reversible transformation between basic covalent bond (CB) and exited **alternative bond (AB)**: $\Sigma\Sigma(CB \leftrightarrow AB)$.

The bond wave “elementary cell” is just shown in Fig.2c, where alternative bonds are considered as three-center bonds (TCB) in accord with the early model of hypervalent bonds after Dembovsky [4]. The following quantum-chemical study of “glassy” bond revealed concrete hypervalent bonds in typical

glass formers (see review [5]); however, the nature of AB is insignificant now, as well as the network motive: 1D (like Se), 2D (like B₂O₃) or 3D (like SiO₂).

From a historical point of view, the bond wave model was born in the middle of 1980s owing to our magneto-viscous experiments [6,7], whose features – the field weakness and diamagnetic nature of glass – cannot be explained in frames of classical physics. Fortunately, the self-organization approach was developing intensively just then, but unfortunately, not in glass science, a fact that forced me to choose a roundabout way to meet glass community with the bond wave idea.

In doing so, I have used common thermodynamic data, phase transitions temperatures (T_m and T_b) and atomization energy (E_a), to construct the $T_m=f(E_a)$ and $T_b=f(E_a)$ plots for “normal”, molecular, and glass-forming substances [19]. Molecular substances, as expected, fall far below the “normal” lines. The fall of glass-formers is much less but remains strong enough to be neglected. For example:

Table 1. Atomization energy and phase transition temperatures for Se and SiO₂: real (T_m and T_b) and predicted (T_m^* and T_b^*)

	E_a , kcal/g-at	T_m , K	T_m^* , K	T_b , K	T_b^* , K
Se	52	494	940	958	1550
SiO ₂	149	1883	2700	2503	4400

This fact points to a substantial *inhomogeneity* in chemical bonding for two falling groups. Molecular substances are composed of strong covalent bonds within the molecules and very weak van-der-Waals bonds acting between them, so even a light heating leads to destruction of a molecular crystal; firstly at T_m , above which the temporarily closing molecules are linked with van-der-Waals bonds that switch from some atoms to others, and then at T_b , when van-der-Waals bonds break totally releasing free molecules into the gaseous phase.

Covalently bonded crystal endures thermal stress far longer, up to a relatively high “normal” temperature T_m^* , above which the system of covalent bonds destroys totally because of metallization of bonding. Ideal metallic bond represents a positively charged frame united by a negatively charged cloud of electrons. Corresponding covalent-to-metal transition of bonding is observed by electric conductivity as the *insulator-to-metal* or *semiconductor-to-metal* types of melting.

In contrast to “normal” crystals, the glass-forming ones does not metallize at melting. A simple example are crystals of chalcogen group – S, Se, Te. Tellurium, being the non-glass-forming substance, is known to metallize continuously when heating above T_m [20], whereas glass-forming selenium and sulfur demonstrate the *semiconductor-to-semiconductor* transition [21] thus demonstrating conservation of covalent network in the molten state. This feature, which is known as the “polymeric” structure of glass-forming melts, does not explain, however, why covalent network become mobile after melting. The puzzle can be resolved by means of alternative bonds and their wavelike self-organization in the following way.

A crystal of glass-forming substance can avoid metallization at heating by transformation a piece of covalent bonds into higher-energy alternative bonds at a sufficiently low temperature $T_m < T_m^*$ (Fig.1, Table 1). The process develops until concentration of alternative bonds reaches a critically high level when they can “feel” each other by means of local elastic fields generated in covalent network around each “alien” bond. Then alternative bonds gather into the layers, and the closed layers organize the 3D bond wave. The thermal energy absorption at melting includes formation of more and more effective *dissipative patterns*: first by isolated alternative bonds, then by their 1D aggregates (strings) and 2D aggregates (layers), and finally by 3D bond wave whose wavefronts, the collectively moving layers, complete transformation of crystalline network into the non-crystalline one as a suitable medium for free moving of the 3D bond wave.

Disappearance of crystalline order does not mean, however, disappearance of order at all. Moreover, a richer *hierarchical* order appears. Let us illustrate this by means of Fig.2c which shows *three* characteristic orders of different length/scales. The scale of *short-range order*, SRO, is defined by the length of covalent bond marked as short lines between white atoms; this length is 2.3\AA for Se (Se-Se), 1.7\AA for SiO_2 (Si-O), etc. The SRO length can be extracted also from structural experiment as a radius of the *first coordination sphere*, $R_1 \approx 2\text{\AA}$, which is obtained by means of Fourier transformation of initial diffraction picture.

The initial picture gives information about the *medium-range order*, MRO, observed as the *First Sharp Diffraction Peak* (FSDP). The MRO length corresponds to the wavefront thickness $d = 2\pi/Q_1 \approx 4-6\text{\AA}$, where Q_1 is the FSDP position. Just a system of equidistant wavefronts, two of which are shown in Fig.2c, give a relatively strong and *sharp* reflex. One can find other details about FSDP/MRO in my articles [12, 22-25].

The most intriguing is the *non-crystalline long-range order*, NC-LRO, in the form of Λ -lattice whose “elementary cell” is shown actually in Fig.2c. Unfortunately, Λ -lattice

cannot be detected by ordinary X-ray analysis using $\lambda = 1-2\text{\AA}$ because of a strong parasitic scattering in the low- Q region; the synchrotron radiation of varying λ is an alternative. Fortunately, a simple indirect observation is possible just now by fractography, as it will be demonstrated in Section V. But before let us consider two aspects of the bond wave model, conditionally theoretical (III) and experimental (IV).

III. ORDER PARAMETER – THE WAVELENGTH

To estimate the bond wave parameters as a function of temperature, let accept for simplicity the activation law for concentration of alternative bonds, namely,

$$N = N_0 \cdot \exp(-\Delta\varepsilon/kT) \quad (1),$$

where $\Delta\varepsilon$ is the energy difference between the excited (AB) and the ground (CB) bonding states, and N_0 is a pre-exponent.

From Fig.2c it follows

$$N/N_S = d/\Lambda \quad (2),$$

where N_S is the AB concentration in d -layer.

By combining of Eq.(1) and Eq.(2), one obtains the temperature dependence of the bond wave *wavelength*

$$\Lambda = \Lambda_3 = d \cdot (N_S/N_0) \cdot \exp(\Delta\varepsilon/kT) \quad (3).$$

Note that Λ_3 relates to the *three-dimensional* bond wave corresponding to region ‘I’ on the top part of Fig.3; other regions will be considered some later.

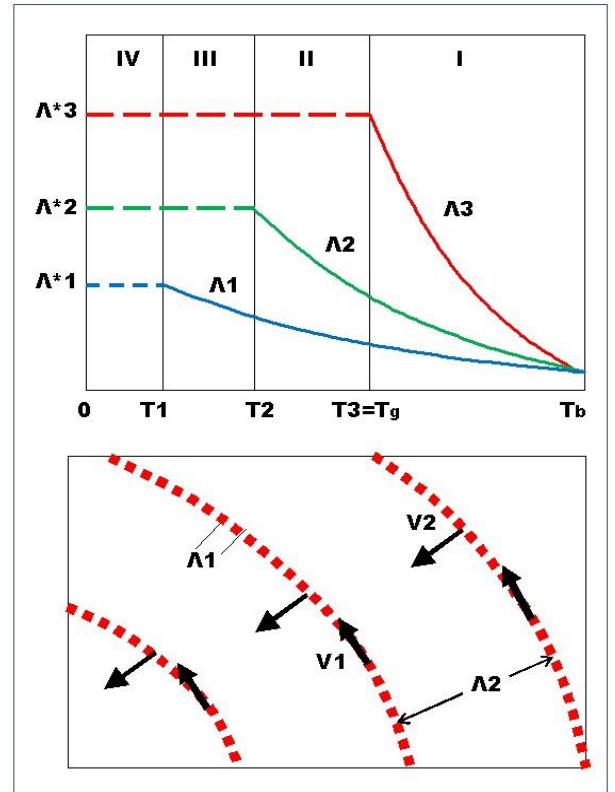


Figure 3. Temperature dependence of the wavelengths (top), and the 2D and 1D bond waves (bottom).

Bond wave dissipates thermal energy by *moving* through the network with a temperature-dependent **velocity** defined as $V(T)=f(T)\cdot d$, where $f(T)\sim\exp(-\varepsilon_f/kT)$ is frequency of the temperature activated “jumps” ($AB\rightarrow CB\rightarrow AB$, etc.), d is the wavefront thickness (**Fig.2c**), and ε_f is the jumping barrier. The reader can find numerical evaluation of $V(T)$ for Se in Ref.26. Despite of the same *exponential* temperature dependence for the velocity and the wavelength, $\Lambda(T)$ and $V(T)$, they change in the *opposite* way, so that when heating, wavelength decreases and velocity increases, and much faster since $\varepsilon_f > \Delta\varepsilon$ (barrier is greater than corresponding difference in levels).

Now let us heat a melt from T_m . The wavelength of 3D bond wave decreases up to a critical temperature T_b when the wavefronts become in contact ($\Lambda=3d$), so the network becomes homogeneous ($N=N_s$), and the bond wave *disappears*. This is situation of **boiling**, when alternative bonds belonging to the osculated wavefronts interact with explosive breaking, and free covalent fragments escape into the gaseous phase.

In the opposite process of melt cooling, 3D bond wave reaches the second critical point, T_3 , when the critically distant wavefronts cannot “feel” each other by means of elastic field generated by them in surrounding covalent network. A feedback between the wavefronts breaks, and 3D bond wave stops, being *freezing* in the network in the form of Λ^*3 -lattice. As far as the *volume* mobility of a liquid is provided by the 3D bond wave, this freezing corresponds to **glass transition**; so $T_3=T_g$ and $\Lambda^*3=\Lambda_g$, as it is shown on the top part of **Fig.3**.

The 2D and 1D bond waves, representing respectively collective/mobile “strings” in the limits of each d -layer and collective alternative bonds in the limits of each string, remains refrozen below T_g , as it is shown in the bottom part of **Fig.3**. Nevertheless, these low-dimensional waves also freeze at related temperatures T_2 and T_1 . Below T_1 glass is completely “dead” in the sense that every mobility provided by the bond waves is arrested there.

Fortunately, the low-temperature “death” of glass is *reversible* owing to thermal generation of alternative bonds and their ability for integration. When *heating*, there refreeze successively 1D bond wave at/above T_1 , the 2D bond wave at/above T_2 , and finally the 3D bond wave at/above $T_3=T_g$. If the freezing/refreezing processes are not symmetrical (compare with braking/racing of a car), one can explain the phenomena of *hysteresis*, and not the well-known hysteresis around T_g (e.g., [8, p.29]) but also those at T_2 and T_1 . Corresponding two hysteresis may be discovered when studying low-temperature properties and/or the so-called “*secondary relaxation*”.

Now one can distinguish now four temperature regions for glass-forming liquid and glass.

Region I: Viscous liquid (T_g-T_b). All three bond waves (1D, 2D, 3D) coexist, and the region specificity is determined by 3D bond wave which animates all the volume and thus appears in “macroscopic” processes, *viscous flow* first of all.

Region II: Plastic glass (T_2-T_g). Below $T_3=T_g$ concentration of alternative bonds in the frozen wavefronts remain high enough for realization of 2D bond waves which spreads along the stopped d -layers, thus providing 2D processes like *plastic flow* by sliding of d -layers under stress.

Region III: Brittle glass. Because of freezing of the 2D bond waves, glass enters the “brittle” region, when plastic flow and other 2D processes are arrested. A single response to mechanical stress is destruction of glass article, a fast process that denudes the frozen d -layers as the regions populated with a relatively weak alternative bonds; the jumping between the layers can be observed by characteristic *conchoidal fracture*.

Region IV: “Dead” glass. This hypothetical state is the most hard and immobile because of freezing of the bond waves of every dimension. An *explosive destruction* is expected here.

IV. ATTRACTOR FOR THE VISCOSITY-TEMPERATURE BEHAVIOR

Let us begin from **Region I** that corresponds to viscous liquid. The well-known feature of the glass-forming liquids is their *non-Arrhenius* behavior, which one can see even in GeO_2 (**Fig.4a**), a typical “strong” liquid in terms of the strong-fragile classification after *Angell* [30].

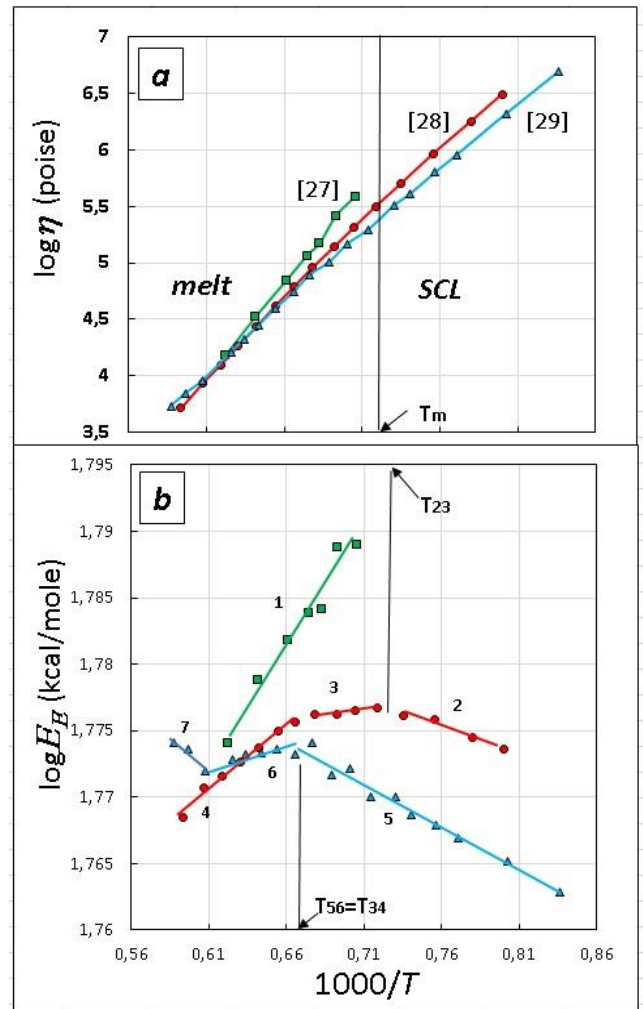


Figure 4. Experimental viscosity-temperature data for GeO_2 after *de Neufville et al* [27, Pt viscometer] (line 1), *Fontana & Plummer* [28, Run 1] (lines 2-4), and *Bruckner* [29] (lines 5-7) presented in the *Arrhenius* plot (a) and in the *TA*-plot (b).

Let us define as “ideal strong” a hypothetical liquid that obeys the Arrhenius equation

$$\eta(T) = \eta_{\text{Arr}} \cdot \exp(E_{\text{Arr}}/RT) \quad (4)$$

with $\eta_{\text{Arr}} = \text{const}$ and $E_{\text{Arr}} = \text{const}$. When using Eq.(4) for a real liquid, both parameters become temperature dependent. To avoid excess variables, we have proposed earlier [31] to use the Eyring [32] equation

$$\eta(T) = \eta_E \cdot \exp(E_E/RT) \quad (5),$$

in which only E_E , the **Eyring activation energy**, depends on temperature since $\eta_E = Nh/V$ (N and h are the Avogadro’s and Plank’s constants, and V is the molar volume) is practically constant in a wide temperature range because the temperature dependence of density, $\rho \sim 1/V$, is negligible as compared with that for viscosity. Moreover, all glass-formers have practically the same $\log \eta_E \approx -4$. Thus, the many-factor analysis of the viscosity-temperature data can be substitute for the $E_E = f(T)$ analysis irrespectively of the liquid “fragility” [33]. The analysis includes three steps of an increasing generality.

1. TA plot $\rightarrow \Sigma\{A_i; G_i\}$

First, a set of experimental $\eta(T)$ points transforms into the $E_E(T)$ set by means of the following calculation formulas:

$$E_E \text{ [kcal/mole]} = (4573/T) \cdot [\log \eta(T) - \log \eta_E] \quad (6)$$

$$\text{and } \eta_E \text{ [poise]} = 0.0039 \rho \text{ [g/cm}^3\text{]} / M \text{ [g]} \quad (7),$$

where ρ is average density and M is molecular weight; $\log \eta_E$ is equal to -4.0 for GeO_2 , -3.8 for SiO_2 , -3.65 for Se , etc.

Second, the $E_E(T)$ set is presented in “activation” coordinates, i.e., $\log E_E(T) = 1/T$, as it is shown for GeO_2 in **Fig.4b**. The plot call “**twice activation**” (TA) since it is *activation* plot for *activation* energy. When doing so, the difference between three sets of experimental data [27-29] becomes enormous and looks not an “error”. Each $E_E(T)$ set can be approximated by a line or few lines described by equation

$$\log E_{Ei} = A_i \cdot \exp(G_i/RT) \quad (8).$$

A set of the $\{A_i; G_i\}$ pairs for the considered liquid creates a basis for the second step.

2. Master plot $\rightarrow \{a; b\}$

Although disposition of the TA-lines in **Fig.4b** looks chaotical, they prove interconnected by their $\{A_i; G_i\}$ parameters, being linearizing in the semi-logarithmic coordinates, as it is demonstrated in **Fig.5** for GeO_2 . The line equation

$$\log A = a - b \cdot G \quad (9),$$

gives the next pair $\{a; b\}$ which characterize the viscosity-temperature behavior of a liquid irrespectively of a concrete experiment. All glass-forming liquids analyzed by me so far demonstrate the same behavior characterized numerically in **Table 2**. Therefore, one can formulate the **principle of partial reproducibility** for the viscosity-temperature data that calls:

viscosity of a glass-forming liquid does not defined strictly by temperature, the only one necessary demand for experimental $\eta(T)$ being concordance to the previously defined **convergence point $\{a; b\}$** for the liquid considered. In terms of self-organization, convergence point represents **attractor** for the viscosity-temperature behavior.

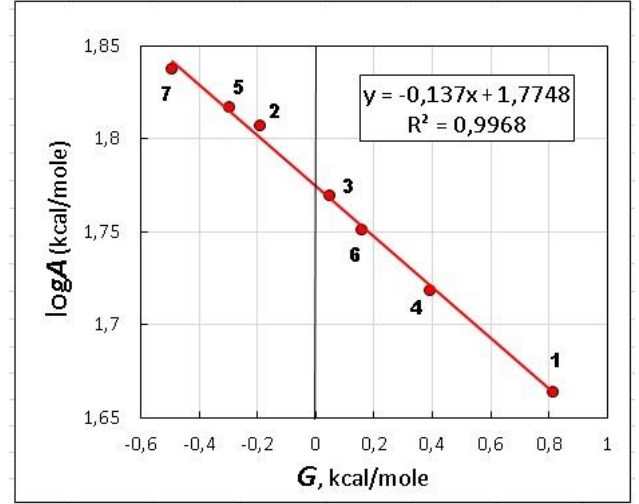


Figure 5. Master plot for GeO_2 . The point designation corresponds to the TA-lines in **Fig.4b**.

Table 2. Viscosity-temperature behavior for typical glass-forming liquids; fragility m by Eq.(11), η in [poise], a and b correspond to the [kcal/mole] dimension for A and G in Eq.(9).

Liquid	T_g, K T_m, K	m $\log \eta(T_m)$	a b	Ref. for $\{a; b\}$
SiO_2	1500	18	2.014	28, 29
	1983	7.8	0.101	
GeO_2	880	18	1.775	27-29
	1389	5.5	0.137	
B_2O_3	560	40	1.486	34
	748	4.8	0.298	
Se	310	55	1.324	35, 36
	494	1.6	0.700	
Gly	190	60	1.136	37, 38
	291	1.1	1.202	

A consequence of partial reproducibility is a little importance of searching “true” $\eta(T)$, as well as of construction of a *general* viscosity-temperature equation, a “Holy Grail” for generations of glass scientists. Instead these equations with an increasing number of fitting parameters, I propose the *universal* one-variable ($A_i = \text{var}$) equation

$$\log \eta(T)_i = \log \eta_E + (A_i/2.303 RT) \cdot \exp\{[(a - \log A_i)/b]/RT\} \quad (10)$$

suitable for every liquid with the known convergence point.

3. Convergence plot $\rightarrow \Sigma\{a;b\}$

One can note in **Table 2** definite interrelations between the values of coordinates of convergence point. (a and b change in opposite direction) and between coordinates and m , the index of fragility [30], defined as

$$m = |d(\log \eta(T)/d(T_g/T))|_{T_g} \quad (11).$$

These tendencies become obvious in **Fig.6**, where two branches, one for “fragile” liquids (Se, glycerol) and another for “strong” ones (GeO_2 , SiO_2) appear; “intermediate” B_2O_3 locates near intersection of the branches.

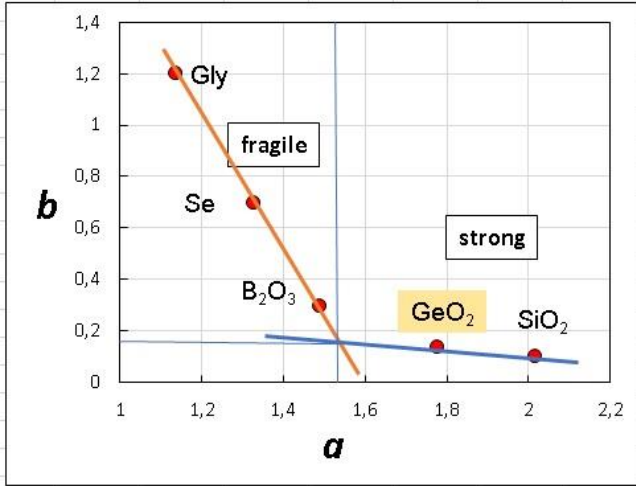


Figure 6. Convergence plot for the liquids listed in **Table 2**.

Of course, the convergence plot needs a more detailed investigation that can lead in turn to a more general classification of glass-forming liquids, which is a subject of my next paper. Now let us remain to self-organization and consider HOW a liquid “knows” what a $\eta(T)_i$ would realize during a concrete measuring of viscosity? This is a part of general problem of how *adaptation* of a self-organization system (including us) to environment proceeds.

V. INFORMATION FIELD FOR THE BOND WAVE

Information as an instrument for adaptation of an object to its medium is a central point of self-organization [39, 40]. In the glass-forming case, it needs an *information field* that gives the *direction* for the bond wave spread. What is more, information field is a necessary condition for *glass formation* itself just because when the bond wave does not “know” where to run it cannot realize at all; in addition, there is no the dissipative pattern except 3D bond wave that can transform the long-range order of initial crystal to the non-crystalline order, as it was described above in Section II.

The adaptation ability of a substance is maximum above T_g , where 3D bond wave animates all the structure, and decreases at cooling both continuously and in the step-type manner when 3D, 2D and 1D bond waves freeze successively in accord with **Fig.3**. The 3D adaptation during measurement of viscosity is illustrated by **Fig.7**, where the process of option

of successive viscous patterns realizes the *feedback loops* between “substance” and “information” columns.

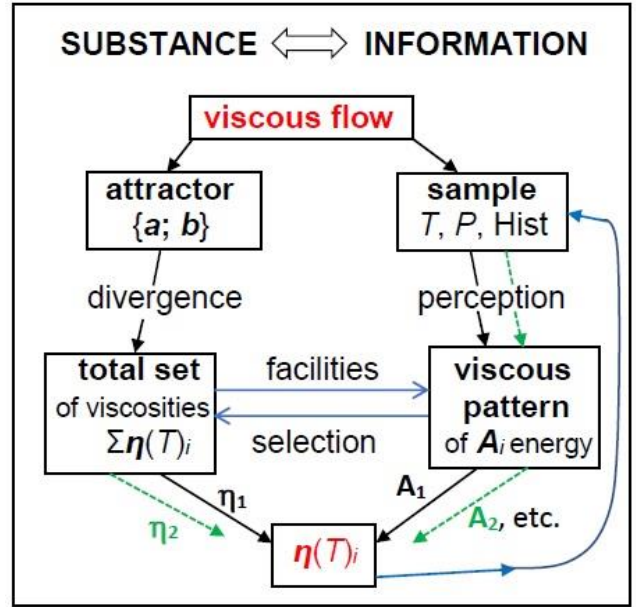


Figure 7. Self-organization at viscous flow of a sample depending on the sample composition (substance), temperature (T), pressure (P), and history ($Hist$).

Information field acting at viscous flow is the pressure gradient, $\text{grad}P$, generated by viscometer. A more complex case of two information fields, pressure and temperature gradients, ($\text{grad}P + \text{grad}T$), is shown in **Fig.8**.

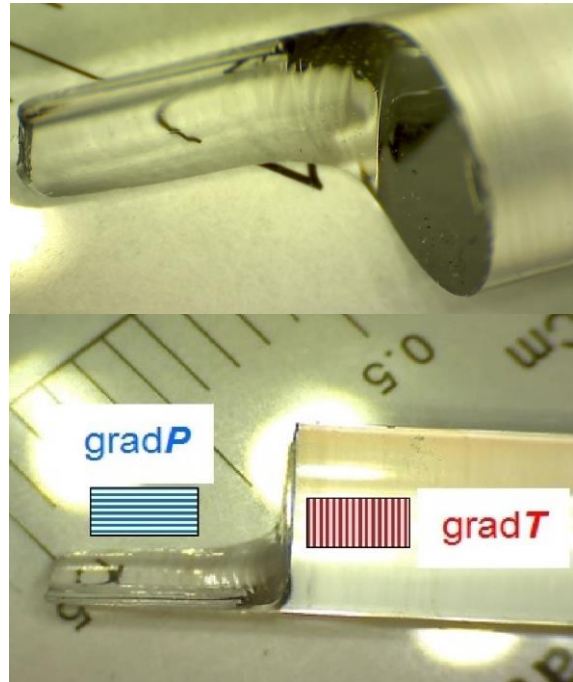


Figure 8. The frozen wavefronts of two bond waves directed previously by the temperature and pressure gradients.

Glassy rod, which was obtained by drawing from a softening ingot, was influenced by the temperature gradient (**gradT**) from a heater and the pressure gradient (**gradP**) from a drawing device. This combination of information fields presents in every process of glass making. The *frozen* wavefronts which are denuded by fracture in **Fig.8** demonstrate the **solitonic** behavior of corresponding 3D bond waves, i.e., their ability to intersect without distortion.

Fractography creates a remarkable possibility to observe bond waves almost *in situ*, at least for the situation existing during/before solidification when 3D bond waves were freezing. This possibility helps to understand the action of other information fields such as *magnetic* field considered below.

Table 3. List of the field effects studied in our laboratory; **=H** and **~H** correspond to constant and pulsed magnetic field, **US** correspond to ultrasonic field in the cavitation regime.

IF	Substance	Property	General effect	Ref.
=H 240Oe	Se	Viscosity (in situ)	$\Delta \lg \eta^H = \pm 0.2$ <i>Anisotropy</i>	[6]
~H 240Oe, 50 Hz	Se	Viscosity (in situ)	Resonance $\Delta \lg \eta^H = +0.3/-0.5$ <i>Anisotropy</i>	[7]
=H 240Oe	As ₂ S ₃	Color Fracture	<i>Red shift</i> for the “magnetic” sample (MS); <i>Plane</i> for MS (Fig.9)	[41]
US 0.3 W/cm ²	Se-Te	Optical transmission spectra.	<i>Non-linear</i> change in Se-X series of glasses; <i>Anisotropy</i> .	[42]
	Se-As			[43]
	Se-S	SEM	Unusual images; <i>Anisotropy</i> (Fig.11)	[44]
	Se:Cl			[45]

First experiment in **Table 3** concerns viscous flow of softening Se glass under the action of a **constant magnetic** field [6]. It was initiated by *Dembovsky* who has expected to observe the proposed hypervalent bonds to form charged “defects” for *switching* covalent bonds from some atoms to others [4]; viscous flow as a collective switching represents an electric current which can interact with magnetic field thus influencing viscosity. The effect was really obtained, however, it was doubtful because of (1) *diamagnetic* nature of glass and (2) *weakness* of the field whose energy is negligible as compared with thermal energy ($\mu_B H \ll kT$), so thermal motion should reorient the current. Unfortunately, a relatively small value of the effect, $\Delta \lg \eta \approx 0.2$, which is of the order of a possible experimental error of measuring viscosity, confirms the rejection of this unusual effect.

In attempts to increase the effect value, we have tested the **pulsed** magnetic field of technical **50 Hz** frequency and the

same intensity. First the effect was disappeared at all, however, after scanning of temperature has appeared again in the form of a strong **viscosity-temperature resonance**, $|\Delta \lg \eta^H| \rightarrow 0.5$ at **321K** [7]. This value is too high to be neglected, nevertheless, being remaining impossible from the “classical” point of view.

The first step to understand the magneto-viscous effects was assumption about the *one-electron* transition state B* arising at the elementary act of bond exchange (CB \leftrightarrow B* \leftrightarrow AB) [46]. This can explain the magnetic field influence on elementary processes but not on the macroscopic ones like viscous flow. The bond wave like a macroscopic formation permits to solve this problem. Really, magnetic field can interact with a collective of wavefronts that become magneto-active when “jumping” in the wave direction, and interaction becomes especially effective when the frequency of collective “jumps” of the wavefronts, $\Sigma(CB \leftrightarrow B^* \leftrightarrow AB)$, coincides with the field frequency, a situation that realizes for Se in the 321K//50 Hz point determined in our experiment [7].

As far as magnetic field acts as *information field*, its intensity is not matter above the field threshold, which was defined to be as low as 150 Oe [6]. Acting on the wavefronts jumping, magnetic field tend to *orient* bond wave in the field direction, thus facilitating (in longitudinal field) or hampering (in the transverse field) viscous flow – in accord with *anisotropy* of the effect observed in solenoid and electromagnet, respectively.

In the above experiments there are two information fields: *elastic* field generated by viscometer and *magnetic* field correcting the flow. To extract the magnetic field action, I have proposed to prepare the “magnetic/non-magnetic” pairs of Se, As₂Se₃ and As₂S₃ glasses [47]. The last was a lucky choice because of immediate change in color: from natural red to almost black in “magnetic” sample, as it is seen in **Fig.9**.

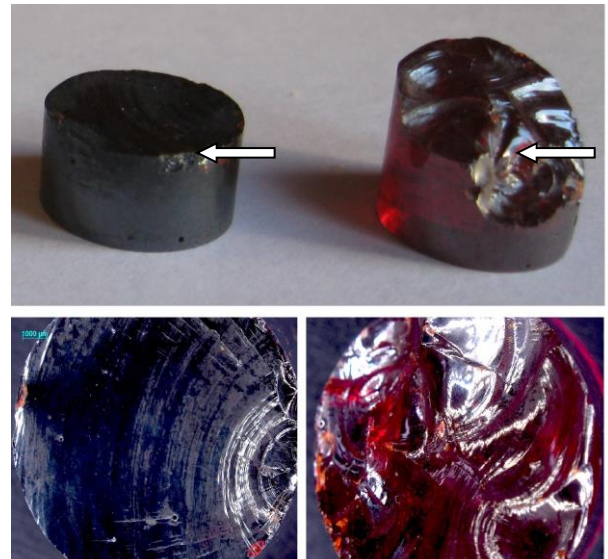


Figure 9. The fractured samples of “magnetic” (on the left) and “non-magnetic” (on the right) As₂S₃ glasses; a sight from sideways (top) and from above (bottom).

The second difference emerged ten years later [41], after splitting As_2S_3 samples in the middle, as it is shown by white arrows in **Fig.9**. To understand the both differences, let us stop on the details of experiment. help to understand the results. The samples of each pair were prepared at the same conditions, namely, by melting of industrial As_2S_3 glass in evacuated quartz ampules at 450°C for 1 hour in a tube furnace placed inside electromagnet with the following cooling for 20 min inside the cut off furnace up to room temperature. The 240 Oe magnetic field was applied to the “magnetic” sample *during all the melting/cooling process*.

On the first glance, the observed effect of the magnetic treatment conflicts with the bond wave model. Really, the *transversal* field of electromagnet should orient the wavefronts *along* the sample/tube axis and not across, as it is observed. Besides, the darkening of “magnetic” sample remains a puzzle.

Nevertheless, the bond wave model can overcome the challenge when taking into account the bond wave dimensionality (**Fig.3**). When cooling of the homogenized melt, there realized initially 3D bond wave(s), which remains the main dynamic factor up to enter the glass transition region. Magnetic field tend to orient the wavefronts/layers in the field direction, i.e., *along* the sample axis. A critical situation appears in the softening glass, some above T_g , where 3D bond wave becomes weaker (collective *d*-layers are stopping in the network) while 2D bond waves (collective strings on *d*-layers) remains quite active. Magnetic field tend to orient the strings along the field lines, i.e., across the 3D bond wave direction. As a result, the *d*-layers tend to *rotate* in the freezing covalent network. The fractures observed in **Fig.9** indicate that 2D bond waves has won the battle: all the frozen *d*-layers in “magnetic” sample are oriented by electromagnet *across* the sample axis.

As to the darkening of “magnetic” sample, it can be compared with the well-known *red-shift* of optical edge observed after laser irradiation of chalcogenide films at $T \ll T_g$; this “*photostructural change*” was interpreted by us earlier [48] as “loosening” of covalent network because of the light-induced collective drift of the chemical-bond “defects” in it. Similarly, we observe here the red-shift due to “loosening” of solidifying network of As_2S_3 by means of rotating *d*-layers.

Finally, let consider a complex *conchoidal* fracture of “non-magnetic” sample shown in the right part of **Fig.9**. The fracture reproduces a complex thermal field, $\Sigma \text{grad}T$, that was existing in the solidifying sample. A highly ordered fracture observed in “magnetic” sample indicates that magnetic field has won the “information battle” between *H* and $\Sigma \text{grad}T$.

The last series of information treatments concerns **ultrasonic** (US) field applied in the *cavitation* regime to four Se-X series ($X = \text{Te}, \text{S}, \text{As}, \text{Cl}$) of softening glasses with Se as the main component. It was found previously [49] a strong *non-linearity* in fresh samples, which is manifested by extrema at 1-2%Te, 5%As, 1%S, and 0.01-0.02%Cl on the property-concentration curves; note that non-linear behavior is a feature of self-organizing systems. The option of Se-based glasses gives opportunity to use *water* as the cavitation medium realized by a simple device shown in **Fig.10**. The field intensity about 0.3 W/cm^2 was enough to heat water up to 40°C or 50°C ,

and final “high-temperature” treatment at 72°C was achieved by adding of hot water into the bath during experiment. The treatment time was 2-5 min depending on temperature.

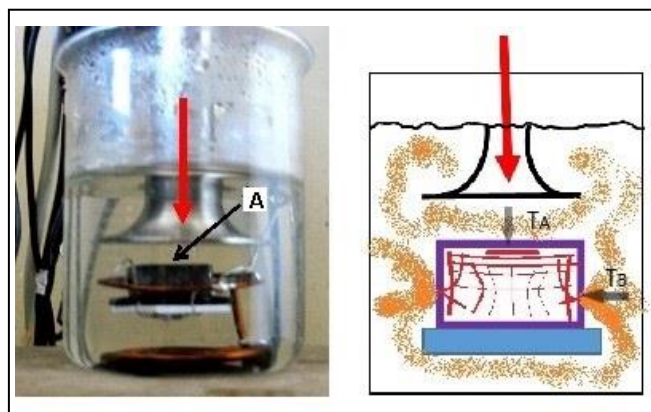


Figure 10. US-treatment of Se-X samples: the cell (on the left) and the scheme of action (on the right). Red arrow is the US input, red curves are the wavefront section. Arrows T_A and T_B indicate two directions for measurement of optical spectra.

The samples of a given Se-X series were measured at room temperature by optical transmission in the $300\text{-}5000 \text{ cm}^{-1}$ range before and after each treatment. The spectrum of Se standard treated in hot water at 72°C for the same time (2 min) was not changed, therefore, we observed not a temperature but a cavitation-temperature effect. We watched in the spectra both specific lines and *transparency*, *T*, defined as optical transmission at 1000 cm^{-1} , a frequency that divides the vibrational region and the “window of transparency” located above 1000 cm^{-1} for selenide glasses.

The details of US-induced effects one can see in original papers [42-45]; they are located at the same “extremal” concentrations which were found in fresh samples [49]. To illustrate characteristic *anisotropy* and *non-linearity* let look at **Fig.11** for initial and “extremal” samples of the Se-Te series.

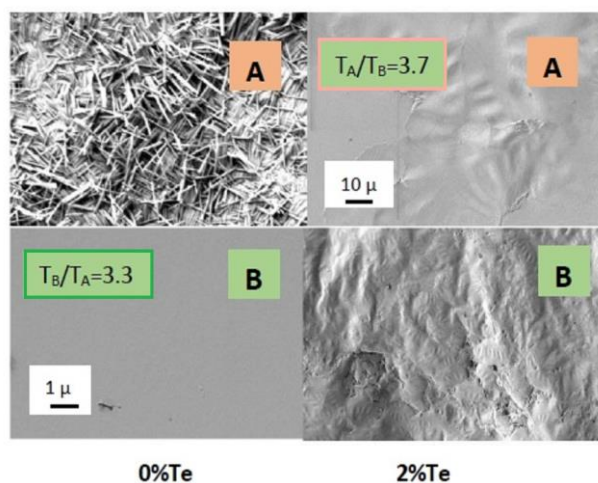


Figure 11. The SEM images for two final Se-Te samples fractured along (A) and across (B) the US input (see **Fig.10**).

All samples became almost “dark” after the 72°C cavitation treatment as concerns very low but measurable transparency; this is the final treatment. The Se-Te samples presented in **Fig.11** were fractured along and across the previous US input shown by red arrow in **Fig.10**, thus denuding **A** and **B** fractures shown in **Fig.11**. While the pre-treated samples were normally isotropic ($T_A=T_B$), final samples demonstrate a strong *optical anisotropy* ($T_A \neq T_B$), however, of the *inverse* character: $T_A < T_B$ for 0%Te and $T_A > T_B$ for 2%Te. This is a sign of *non-linearity* observed previously in the Se-Te series (0, 1, 2, 5, 10%Te) with 1%Te and 2%Te samples as ones of “extremal” composition [49].

Additional data of microstructure in **Fig.11** is especially interesting. Note that all four fractures were looked glassy by the eye (smooth, bright) when observed before SEM. The SEM images look different, except **B**-fracture of pure Se (0%Te), which looks like SEM of a typical glass. However, **A**-fracture of the same 0%Te sample looks like a carpet of “needles”. This difference between the fractures look correlates with their transparency ($T_A < T_B$) as far as needles represent microcrystals that scatter incident beam so decrease transparency (see T_A arrow in **Fig.10**). The problem is Se is known to crystallize in the *spherulitic* manner.

The “extremal” 2%Te sample brings a new puzzle: it demonstrates not only inverse of anisotropy ($T_A > T_B$) but also the “cloudy” species which look neither crystalline nor glassy. Probably, we observe an *intermediate* glass-to-crystal form arising due to cavitation treatment of this “extremal” sample. The problem is that we do not know *when* the observed inhomogeneities, both “needles” and “clouds”, were formed: during cavitation treatment or after, when previously activated samples were cooling in air and keeping before SEM.

The latter possibility emerged because of repeat SEM of Se(0%Te) made after 6 months: the *islands of needles* have developed on the **B**-fracture too. This means that the process of crystallization of the US-treated glass continues below T_g , where only 2D bond waves are active. Note, however, that the *low-temperature* ($T < T_g$) crystallization, which is provided by 2D bond waves, should differ from the *high-temperature* crystallization provided mostly by 3D bond waves at $T > T_g$ not only in kinetics but also in location and morphology [50].

VI. DISCUSSION

The synergetic approach presented here differs from conventional one in general points listed in **Table 4**. The points are considered then in frames of four topics: specificity of glass structure, reproducibility of experimental data, nature of glass transition, and potential practical usage.

1. Structure. Vulgar definition of glass as “a solid having no long-range order” means not more than “glass is not a crystal” if ordinary *crystal*-type long-range order (LRO) is meant. In frames of the bond wave model there appears a specific *non-crystalline LRO* (NC-LRO) [51] which coexists naturally with well-recognized medium-range order (MRO) and common short-range order (SRO). The scale of NC-LRO is determined by the wavelength $\Lambda(T)$, and the scale of MRO – by the wavefront thickness d , as it is illustrated in **Fig.2c**.

When cooling of supercooled liquid ($T < T_m$) there appears a *competition* between 3D bond wave, which supports NC-LRO, and a general tendency to establish “normal” crystal-type LRO below T_m . Every event of glass formation means that 3D bond wave has won this battle with a final solidification of supercooled liquid below T_g .

Table 4. Glass paradigms reconsidered.

GLASS	Conventional notions	The Bond Wave model
Long-Range-Order	Absent	NC-LRO in the form of Λ -lattices
Chemical Bonding	One-state: covalent bond	Two-state: $CB \leftrightarrow AB$
Reproducibility at $T > T_g$	Total, depending on temperature	Partial, depending on glass history
Glass Transition	Various models and theories	3D BW \rightarrow 2D BW transition at T_g
Glass Structure	Models/theories based on CRN	Hierarchical: SRO/ /MRO/NC-LRO
Management of Properties by...	...Chemical Composition	...Composition and Information Fields
Glass Definition	Non-crystalline solid obtained by cooling from melt at a sufficiently high rate (critical cooling rate)	Non-crystalline solid obtained from a liquid possessing self-organization ability in the form of the bond waves

Abbrevitures: CB – covalent bond, CRN – continuous random network, NC-LRO – non-crystalline long-range order, AB – alternative bond, BW – bond wave, MRO – medium-range-order (known also as IRO – intermediate range order).

2. Reproducibility. Usually, supercooled liquid that realizes in the $T_g < T < T_m$ temperature range is assumed to be in “metastable equilibrium”, a term that implies the existence of a definite relation between a property and temperature, and every appreciable deviation from a “true” property-temperature dependence is scarified as “experimental error”. It was demonstrated, however, a definite *freedom* of the viscosity-temperature behavior, which is *restricted* only by *convergence point* – or *attractor* in terms of self-organization. A search for similar attractors for other properties, as well as the pressure-induced shift of the attractors, opens a new perspective for glass science.

One may connect different viscous patterns with the intensively discussed pressure induced “liquid-liquid” phase transitions (see [52] for introduction), however, this is a very far analogy at present for at least two reasons. First, transition between viscous patterns looks rather chaotic, being depending not only on temperature but also on the sample *history* (**Fig.7**). Second, if one interprets the $\eta(T)_i$ as a “phase”, this is the *dynamic* phase transitions observed at T_{ij} points, here at *normal pressure* (**Fig.4**).

3. Glass Transition is a central point in glass science, being also an object of a permanent discussions for more than a century. The main disagreement concerns a nature of the dramatic loss of mobility below T_g , the glass transition temperature. In frames of the bond wave model, glass transition is the *dimensionality* one: from 3D BW in liquid to 2D BW in solid. As far as 3D bond waves are frozen/stopped below T_g , the *volume* mobility, including viscous flow, is arrested below T_g , where only the low-dimension processes, such as plastic flow along the stopped *d*-layers, remain. This is my answer to the principal question “*why glasses do not flow*” [53]. As to numerous theories/models of glass transition proposed so far, I know the only one that also uses dimensionality – this is the *Ojovan* model for silica which considers a hypothetical system of percolating clusters named “*vitrons*” [54]. This model, however, leads to the *increase* of dimensionality when cooling – from fractal dimensionality $d_f=2.3$ in liquid to Euclidian dimensionality $d=3$ in glass.

4. Practice. It is quite evident that development of technology needs a deeper understanding of the processes implicated. Based on the bond wave model, I propose to use the low-energy *information fields* (IF) for managing of the glass making process. Note that information fields, at least in the form of *temperature and pressure gradients*, always present during the process, and one can use them more effectively when describes underlying bond wave picture. Besides usual information fields, one can introduce additional ones, e.g., *magnetic* and *ultrasound* fields, whose influence on softening bulk glasses was demonstrated in Section V. The same approach can be applied also to thin films, as it was shown in Ref.55 on the example of memory elements based on the switching phenomenon (*electric* IF) and microlenses formed under laser illumination (*electromagnetic* IF).

When using information fields, one should take in mind two implications. First, external field can provide both *energy* – for the bond wave support, and *information* – for giving the wave direction. A simple example is the thermal field of a given intensity (temperature, the energy level) and direction (temperature gradient, IF). Second, there are usually two or more potential information fields, which can *coexist* in the solitonic manner (see **gradT** and **gradP** in **Fig.8**), *interact* (as **gradP** and **H** in our magneto-viscous experiments), and *depress* a competitor (**H** has eliminated **gradT** in the “magnetic” sample – **Fig.9**). Besides, a possible post-action of IF should be also considered (see last comments to **Fig.11**).

VII. CONCLUSIONS

A new approach to glass nature that combines classical **self-organization** and the **chemical bond** theory in terms of the “glassy” bonds after *S.A. Dembovsky* (1932-2010) is proposed. This approach realized in frames of the **bond wave** model, which is applied successively to experimental data, both known and original, and leads to nontrivial notions about (1) *non-crystalline long-range order*, (2) *partial reproducibility* of experimental data, and (3) *information fields* as a necessary condition for glass formation and a perspective instrument for managing of glass properties.

At present, the bond wave model concentrates on the wavefronts, so on a relatively small (but exceptionally active!) piece of structure. However, since the wavefronts pass through every point/atom, the “*secondary*” **self-organization** in the most of structure may appear, thus linking the “topological” [15] and the “bond wave” aspects of self-organization.

REFERENCES

- [1] H. Haken. Synergetics. An Introduction (3rd ed). Springer, Berlin-Heidelberg, 1983.
- [2] I. Prigogine. From Being to Becoming. Freeman, San Francisco, 1980.
- [3] W. Zhang. Selforganizology: The Science of Self-Organization. World Sci. Publ., Singapore, 2015.
- [4] S. A. Dembovsky. The connection of quasidefects with glass formation in the substances with high lone-pair electron concentration. Mater. Res. Bull. 16 (1981) 1331.
- [5] S. A. Dembovsky, E. A. Chechetkina. Glassy materials clarified through the eyes of hypervalent bonding configurations. J. Optoe. Adv. Mater. 3 (2001) 3.
- [6] S. A. Dembovsky, S. A. Kozyukhin, E. A. Chechetkina. The experimental observation and investigation of defects in glass forming substances with selenium as an example by viscometry in magnetic and electric fields. Mater. Res. Bull. 17 (1982) 801.
- [7] S. A. Dembovsky, E. A. Chechetkina, S. A. Kozyukhin. Anomalous effect of weak magnetic fields on diamagnetic glassy semiconductors. JETP Lett. 41(1985) 88.
- [8] J. Zarzycki. Glasses and the Vitreous State. Cambridge University Press, Cambridge, 1991.
- [9] A. K. Varshneya. Fundamentals of Inorganic Glasses (1st ed.). Academic Press Inc., 1993.
- [10] W. H. Zachariasen. The atomic arrangement in glass. J. Amer. Chem. Soc. 54 (1932) 3841.
- [11] H. A. Robinson. On the structure of vitreous SiO₂ – I. A new pentagonal dodecahedral model. J. Phys. Chem. Solids 26 (1965) 209.
- [12] E. A. Chechetkina. Is there a relation between glass-forming ability and the first sharp diffraction peak? J. Phys.: Cond. Mat. 7 (1995) 3099.
- [13] Z. Shemer, V. Halpern. Correlated weak bonds as a source of the Bozon peak in glasses. (2006) arXiv: 0604714v1.
- [14] J. C. Phillips. Realization of a Zachariasen glass. Solid State Comm. 47 (1983) 203.
- [15] P. Boolchand, G. Lucovsky, J. C. Phillips, M. F. Thorpe. Self-organization and the physics of glassy networks. Philos. Mag. 85 (2005) 3823.
- [16] J. C. Mauro. Topological constraint theory of glass. Amer. Ceram. Soc. Bull. 90 (2011) 31.
- [17] M. Bauchy. Topological constraint theory and rigidity of glasses. (2020) arXiv: 2005.04603.
- [18] P. Boolchand, D. G. Georgiev, B. Goodman. Discovery of the intermediate phase in chalcogenide glasses. J. Optoe. Adv. Mat. 3 (2001) 703.
- [19] E. A. Chechetkina. Rawson’s criterion and intermolecular interactions in glass-forming melts. J. Non-Cryst. Solids 128 (1991) 30.

- [20] A. S. Epstein, H. Fritzsche, K. Lark-Horovitz. Electrical properties of tellurium at the melting point and in the liquid state. *Phys. Rev.* 107 (1957) 412.
- [21] A. M. Regel, V. M. Glazov. Physical properties of electronic melts. (in Russ.) Nauka, Moscow, 1980.
- [22] E. A. Chechetkina. The first sharp diffraction peak in glasses and the other amorphous substances. *J. Phys.: Cond. Mat.* 5 (1993) L527.
- [23] E. A. Chechetkina. Synergetic model for the first sharp diffraction peak in amorphous substances. *Solid State Comm.* 87 (1993) 171.
- [24] E. A. Chechetkina. Medium-range order in amorphous substances: A modified layer model. *Solid State Comm.* 91 (1994) 101.
- [25] E. A. Chechetkina. Self-organization in glass: The synergetic chemical bonding approach. *J. Optoe. Adv. Mater.* 18 (2016) 44.
- [26] E. A. Chechetkina. *Glassy State Clarified from the Eyes of Self-Organization*. Amazon Kindle Direct Publishing, 2019.
- [27] J. P. de Neufville, C. H. Drummond III, D. Turnbull. The effect of excess Ge on the viscosity of GeO₂. *Phys. Chem. Glasses* 11 (1970) 186.
- [28] E. H. Fontana, W. A. Plummer. A study of viscosity-temperature relationships in the GeO₂ and SiO₂ systems. *Phys. Chem. Glasses* 7 (1966) 139.
- [29] R. Bruckner. Physikalische Eigenschaften der oxydischen Hauptglasbildner und ihre Beziehung zur Struktur der Gläser: I. Schmelz- - und Viskositätsverhalten der Hauptglasbildner. *Glastechn. Ber.* 37 (1964) 413.
- [30] C. A. Angell. Relaxation in liquids, polymers and plastic crystals – strong/fragile patterns and problems. *J. Non-Cryst. Solids* 157 (1991) 131.
- [31] E. A. Chechetkina, S. A. Dembovsky. On the form of the viscosity-temperature dependence for glasses and their melts. *J. Non-Cryst. Solids* 105 (1988) 171.
- [32] H. Eyring. Viscosity, plasticity and diffusion as examples of absolute reaction rates. *J. Chem. Phys.* 4 (1936) 283.
- [33] E. A. Chechetkina. Key distinctions in activation parameters of viscous flow for ‘strong’ and ‘fragile’ glass-forming liquids. *J. Non-Cryst. Solids* 201(1996)146.
- [34] T. J. M. Visser, J. M. Stevels. Rheological properties of boric oxide and alkali borate glasses. *J. Non-Cryst. Solids* 7 (1972) 376.
- [35] S. V. Nemilov, A. O. Ivanov. Viscosity of Se-Ge glasses in the softening range. *Zh. Prikl. Khim.* (J. Appl. Chem., in Russ.) 36 (1963) 2541.
- [36] S. A. Kozyukhin. Rheological properties of selenium and selenium-tellurium in the metastable liquid region. Diss. thesis, Inst. Gen. Inorg. Chem., Moscow, 1991.
- [37] R. L. Cook, H. E. King, Jr., C. A. Herbst, D. R. Herschbach. Pressure and temperature dependent viscosity of two glass-forming liquids: glycerol and dibutyl phthalate. *J. Chem. Phys.* 100 (1994) 5178.
- [38] G. Tammann, W. Hesse. The dependence of viscosity upon the temperature of supercooled liquids. *Z. anorg. Allgem. Chem.* 156 (1926) 245.
- [39] H. Haken. *Information and Self-Organization. A Macroscopic Approach to Complex Systems*. Springer, Berlin-Heldenberg, 2006.
- [40] H. Haken, J. Portugali. *Information and Selforganization: A Unified Approach and Applications*. *Entropy*, 18 (2016) 197.
- [41] E. A. Chechetkina. Fracture and fractals in glasses. In: *Fractal Aspects of Materials*, MRS Proc. 367 (1995). P.397-403.
- [42] E. A. Chechetkina, E. V. Kisterev, E. B. Kryukova, A. I. Vargunin. Crystallization of Se-Te glasses in ultrasonic field. *J. Optoe. Adv. Mat.* 11 (2009) 2029.
- [43] E. A. Chechetkina, E. V. Kisterev, E. B. Kryukova, A. I. Vargunin. Crystallization of Se-As glasses in ultrasonic field according to the optical transmission data. *Inorg. Mater.: Appl. Res.* 2 (2011) 311.
- [44] E. A. Chechetkina, E. V. Kisterev, E. B. Kryukova, A. I. Vargunin, S.A. Dembovskii. Preparation of chalcogenide glass-ceramic materials by ultrasonic treatment of glasses. *Inorg. Mater.: Appl. Res.* 3 (2012) 11.
- [45] E. A. Chechetkina, E. V. Kisterev, E. B. Kryukova, A. I. Vargunin. Influence of ultrasound on crystallization of Se:Cl glasses. *Materialovedenie* (Russ.) No.12 (2012) 3.
- [46] S. A. Dembovsky, E. A. Chechetkina. Resonance phenomena and defects in amorphous selenium. *Philos. Mag.* B53 (1986) 367.
- [47] E. A. Chechetkina, S. A. Dembovsky, S. A. Kozyukhin, *et al.* Influence of weak magnetic and electric fields on the structure of chalcogenide glassy semiconductors. In: *Proc. “Amorphous Semiconductors-84”*, Gabrovo, 1984. P.88-90.
- [48] S. A. Dembovsky, E. A. Chechetkina. Hypervalent bonds as active centers providing photo-induced transformations in glasses. In: *Photo-Induced Metastability in Amorphous Semiconductors* (ed. A.V. Kolobov). Wiley-VCH, Weinheim, 2003. P.299-310.
- [49] S. A. Dembovsky, E. A. Chechetkina, T. A. Kupriyanova. Non-linear influence of impurities on the properties of glassy selenium. *Materialovedenie* (in Russ.) No.4 (2004) 37.
- [50] E. A. Chechetkina. Crystallization in glass-forming substances: The chemical bond approach. In: *Crystallization: Science and Technology* (ed. M.R.B. Andreetta). InTech, Croatia, 2012. P.3-28.
- [51] E. A. Chechetkina. The shape of order in glasses. *Phys. Stat. Sol.* B49 (2012) 2034.
- [52] S. M. Stishov. Melting and polymorphic transitions in liquid. (2024) arXiv :2404.12392v1.
- [53] J.-P. Bouchaud. Why the dynamics of glasses super-Arrhenius? (2024) arXiv :2402.01883v2.
- [54] M. I. Ojovan. Glass formation in amorphous SiO₂ as a percolation phase transition in the system of network defects. *JETP Lett.* 79 (2004) 769.
- [55] E. A. Chechetkina. Photostructural changes and electrical switching in amorphous chalcogenides: Bond waves in thin films. *Nat. Sci.* 10 (2018) 70.